

# Extracting the nuclear symmetry potential and energy from neutron-nucleus scattering data

Xiao-Hua Li,<sup>1,2</sup> Bao-Jun Cai,<sup>1</sup> Lie-Wen Chen\*,<sup>1,3</sup> Rong Chen,<sup>1,4</sup> Bao-An Li,<sup>5,6</sup> and Chang Xu<sup>7</sup>

<sup>1</sup>*INPAC, Department of Physics and Shanghai Key Laboratory for Particle Physics and Cosmology, Shanghai Jiao Tong University, Shanghai 200240, China*

<sup>2</sup>*School of Nuclear Science and Technology, University of South China, Hengyang, Hunan 421001, China*

<sup>3</sup>*Center of Theoretical Nuclear Physics, National Laboratory of Heavy Ion Accelerator, Lanzhou 730000, China*

<sup>4</sup>*Department of Physics, Arizona State University, Arizona 85287-1504, USA*

<sup>5</sup>*Department of Physics and Astronomy, Texas A&M University-Commerce, Commerce, Texas 75429-3011, USA*

<sup>6</sup>*Department of Applied Physics, Xi'an Jiaotong University, Xian 710049, China*

<sup>7</sup>*Department of Physics, Nanjing University, Nanjing 210008, China*

(Dated: July 3, 2018)

According to the Hugenholtz-Van Hove theorem, the symmetry energy and its density slope can be decomposed uniquely in terms of the single-nucleon potential in asymmetric nuclear matter which, at normal density, can be constrained by the nucleon optical model potential extracted from analyzing the nucleon-nucleus scattering data. To more accurately extract information on the symmetry energy and its density slope at normal density from neutron-nucleus scattering data, going beyond the well-known Lane potential, we include consistently the second order terms in isospin asymmetry in both the optical model potential and the symmetry energy decomposition. We find that the strength of the second-order symmetry potential  $U_{\text{sym},2}$  in asymmetric nuclear matter is significant compared to the first-order one  $U_{\text{sym},1}$ , especially at high nucleon momentum. While the  $U_{\text{sym},1}$  at normal density decreases with nucleon momentum, the  $U_{\text{sym},2}$  is found to have the opposite behavior. Moreover, we discuss effects of the  $U_{\text{sym},1}$  and  $U_{\text{sym},2}$  on determining the density dependence of the symmetry energy, and we find that the available neutron-nucleus scattering data favor a softer density dependence of the symmetry energy at normal density with a negligible contribution from the  $U_{\text{sym},2}$ .

PACS numbers: 21.65.Ef, 24.10.Ht, 21.65.Cd

## I. INTRODUCTION

Knowledge about the density dependence of nuclear symmetry energy  $E_{\text{sym}}(\rho)$  is critical for understanding not only the structure and reaction of radioactive nuclei, but also many interesting issues in astrophysics, such as the structure of neutron stars and the mechanism of supernova explosions. Although significant progress has been made in recent years in constraining the  $E_{\text{sym}}(\rho)$ , large uncertainties still exist, even around the saturation density of nuclear matter (See, e.g., Refs. [1–9]). It is thus of critical importance to better understand and reduce the uncertainties in constraints placed on the  $E_{\text{sym}}(\rho)$  based on various model analyses of experimental data.

Recently, based on the Hugenholtz-Van Hove (HVH) theorem [10], it has been shown that both the magnitude of  $E_{\text{sym}}(\rho)$  and its density slope  $L(\rho)$  can be analytically decomposed in terms of the single-nucleon potential in asymmetric nuclear matter [11–13]. Moreover, the more general decomposition of  $E_{\text{sym}}(\rho)$  and  $L(\rho)$  in terms of the Lorentz covariant nucleon self-energies within the relativistic covariant framework has also been obtained [14]. These decompositions help us better understand the underlying isospin dependence of strong interaction con-

tributing to the symmetry energy. They also provide a new and physically transparent approach to extract information about the symmetry energy from certain types of experimental data. In particular, at saturation density  $\rho_0$ , the single-nucleon potentials or nucleon self-energies in asymmetric nuclear matter can be constrained by the nucleon optical model potential (OMP) extracted from analyzing the nucleon-nucleus scattering data. In Ref. [11], indeed, the constraints  $E_{\text{sym}}(\rho_0) = 31.3 \pm 4.5$  MeV and  $L(\rho_0) = 52.7 \pm 22.5$  MeV have been obtained simultaneously by using the phenomenological isovector nucleon OMP from averaging the world data from nucleon-nucleus scatterings, (p,n) charge-exchange reactions, and single-particle energy levels of bound states available in the literature since 1969.

In the usual optical model analyses, however, up to now only the first-order symmetry (isovector) potential, i.e., the Lane potential [15], has been considered. On the other hand, using three well-established models it has been shown recently that the contribution of the second-order symmetry potential to  $L(\rho_0)$  depends on the interactions used and generally it cannot be simply neglected [13]. Unfortunately, to our best knowledge, so far there is no empirical or experimental information on the second-order symmetry potential. It is thus of great importance to extract experimental information about the second-order symmetry potential and examine its effects on the density dependence of the symmetry energy. Here we report results of the first work in this direction.

---

\*Corresponding author: lwchen@sjtu.edu.cn

## II. THEORETICAL FORMULISM

### A. Global neutron optical model potential

The optical model is fundamentally important for many aspects of nuclear physics [16]. It is the basis and starting point for many nuclear model calculations and also is one of the most important theoretical approaches in nuclear data evaluations and analyses. Over the past years, a number of excellent local and global nucleon OMP have been proposed [17–22]. The phenomenological OMP for neutron-nucleus scattering  $V(r, \mathcal{E})$  is usually defined as

$$V(r, \mathcal{E}) = -V_v f_r(r) - iW_v f_v(r) + i4a_s W_s \frac{df_s(r)}{dr} + 2\lambda_\pi^2 \frac{V_{so} + iW_{so}}{r} \frac{df_{so}(r)}{dr} \mathbf{S} \cdot \mathbf{L}, \quad (1)$$

where  $V_v$  and  $V_{so}$  are the depth of the real part of the central and spin-orbit potential, respectively;  $W_v$ ,  $W_s$  and  $W_{so}$  are the depth of the imaginary part of the volume absorption, surface absorption and spin-orbit potential, respectively; the  $f_i$  ( $i = r, v, s, so$ ) are the standard Wood-Saxon shape form factors;  $\mathcal{E}$  is the incident neutron energy in the laboratory frame;  $\lambda_\pi^2$  is the Compton wave length of pion, and here we use  $\lambda_\pi^2 = 2.0 \text{ fm}^2$ .

In this work, to obtain information on the energy dependence of the first-order symmetry potential  $U_{\text{sym},1}$  and the second-order symmetry potential  $U_{\text{sym},2}$  in asymmetric nuclear matter, we extend the traditional phenomenological OMP for neutron-nucleus scattering to include the isospin dependent terms up to the second order in  $V_v$ ,  $W_s$  and  $W_v$ , and they are parameterized as

$$V_v = V_0 + V_1 \mathcal{E} + V_2 \mathcal{E}^2 + (V_3 + V_{3L} \mathcal{E}) \frac{N-Z}{A} + (V_4 + V_{4L} \mathcal{E}) \frac{(N-Z)^2}{A^2}, \quad (2)$$

$$W_s = W_{s0} + W_{s1} \mathcal{E} + (W_{s2} + W_{s2L} \mathcal{E}) \frac{N-Z}{A} + (W_{s3} + W_{s3L} \mathcal{E}) \frac{(N-Z)^2}{A^2}, \quad (3)$$

$$W_v = W_{v0} + W_{v1} \mathcal{E} + W_{v2} \mathcal{E}^2 + (W_{v3} + W_{v3L} \mathcal{E}) \frac{N-Z}{A} + (W_{v4} + W_{v4L} \mathcal{E}) \frac{(N-Z)^2}{A^2}, \quad (4)$$

where  $-(V_0 + V_1 \mathcal{E} + V_2 \mathcal{E}^2) \equiv \mathcal{U}_0(\mathcal{E})$  is the isospin-independent real part of the central potential while  $-(V_3 + V_{3L} \mathcal{E}) \equiv \mathcal{U}_{\text{sym},1}(\mathcal{E})$  and  $-(V_4 + V_{4L} \mathcal{E}) \equiv \mathcal{U}_{\text{sym},2}(\mathcal{E})$  are the first- and second-order symmetry potentials of the real part of the central potential in the optical model, respectively. The shape form factors  $f_i$  is expressed as

$$f_i(r) = \left[ 1 + \exp \left( \left( r - r_i A^{1/3} \right) / a_i \right) \right]^{-1}, \quad (5)$$

with

$$r_i = r_{i0} + r_{i1} A^{-1/3}, \quad a_i = a_{i0} + a_{i1} A^{1/3}. \quad (6)$$

In the above equations,  $A = Z + N$  with  $Z$  and  $N$  being the number of protons and neutrons of the target nucleus, respectively.

### B. Single-nucleon potential decomposition of $E_{\text{sym}}(\rho)$ and $L(\rho)$

The equation of state (EOS) of asymmetric nuclear matter can be written as

$$E(\rho, \delta) = E_0(\rho) + E_{\text{sym}}(\rho) \delta^2 + \mathcal{O}(\delta^4), \quad (7)$$

where  $E_0(\rho)$  is the binding energy per nucleon in symmetric nuclear matter;  $\rho = \rho_n + \rho_p$  is the baryon density and  $\delta = (\rho_n - \rho_p) / \rho$  is the isospin asymmetry with  $\rho_n$  and  $\rho_p$  denoting the neutron and proton densities, respectively;  $E_{\text{sym}}(\rho)$  is the nuclear symmetry energy and around saturation density it can be expanded as

$$E_{\text{sym}}(\rho) = E_{\text{sym}}(\rho_0) + L\chi + \mathcal{O}(\chi^2), \quad \chi \equiv \frac{\rho - \rho_0}{3\rho_0}, \quad (8)$$

with  $L \equiv L(\rho_0) = 3\rho_0 \frac{\partial E_{\text{sym}}(\rho)}{\partial \rho} \Big|_{\rho=\rho_0}$  being the density slope parameter.

In the non-relativistic framework, the single-nucleon energy  $\mathcal{E}(\rho, \delta, |\mathbf{k}|)$  in asymmetric nuclear matter can be expressed generally using the following dispersion relation

$$\mathcal{E}_J(\rho, \delta, |\mathbf{k}|) = \frac{|\mathbf{k}|^2}{2m} + U_J(\rho, \delta, |\mathbf{k}|, \mathcal{E}), \quad (J = n \text{ or } p) \quad (9)$$

where the single-particle potential  $U_J(\rho, \delta, |\mathbf{k}|, \mathcal{E})$  can be expanded as a power series of  $\delta$  as

$$U_J(\rho, \delta, |\mathbf{k}|, \mathcal{E}) = U_0(\rho, |\mathbf{k}|, \mathcal{E}) + \sum_{i=1} U_{\text{sym},i}(\rho, |\mathbf{k}|, \mathcal{E}) (\tau_3^J)^i \delta^i, \quad (10)$$

with the  $i$ th-order symmetry potential defined by

$$U_{\text{sym},i}(\rho, |\mathbf{k}|, \mathcal{E}) = \frac{1}{i!} \frac{d^i}{d\delta^i} \left[ \sum_J \frac{(\tau_3^J)^i U_J(\rho, \delta, |\mathbf{k}|, \mathcal{E})}{2} \right]_{\delta=0}, \quad (11)$$

and  $U_0$  being the single-nucleon potential in symmetric nuclear matter. In the above expressions,  $\tau_3^J$  is the third component of the isospin index and here we use the convention  $\tau_3^n = +1$  and  $\tau_3^p = -1$ . The nucleon mass  $m$  is set to be 939 MeV in the following calculations.

From the HVH theorem [10], the Fermi energy  $\mathcal{E}_F^J$  in asymmetric nuclear matter can be expressed as

$$\mathcal{E}_F^J(\rho, \delta, k_F^J) = \frac{\partial(\rho E)}{\partial \rho_J}, \quad (12)$$

where  $k_F^J$  is the nucleon Fermi momentum expressed as

$$k_F^J = k_F(1 + \tau_3^J \delta)^{1/3}, \quad k_F = \left( \frac{3\pi^2 \rho}{2} \right)^{1/3}. \quad (13)$$

Using Eqs. (7), (9) and (12), one can decompose the symmetry energy in terms of single-nucleon potentials as [11–13]

$$E_{\text{sym}}(\rho) = E_{\text{sym}}^1(\rho) + E_{\text{sym}}^2(\rho), \quad (14)$$

with

$$E_{\text{sym}}^1(\rho) = \frac{k_F^2}{6m} + \frac{k_F}{6} \frac{\partial U_0(\rho, |\mathbf{k}|, \mathcal{E})}{\partial |\mathbf{k}|} \Big|_{k_F} + \frac{k_F}{6} \frac{\partial \mathcal{E}}{\partial |\mathbf{k}|} \Big|_{k_F} \cdot \frac{\partial U_0(\rho, |\mathbf{k}|, \mathcal{E})}{\partial \mathcal{E}} \Big|_{k_F}, \quad (15)$$

$$E_{\text{sym}}^2(\rho) = \frac{1}{2} U_{\text{sym},1}(\rho, |\mathbf{k}|, \mathcal{E}) \Big|_{k_F}. \quad (16)$$

In the above decomposition,  $E_{\text{sym}}^1(\rho)$  represents the kinetic energy part (including the contribution from the isoscalar nucleon effective mass) of the symmetry energy while  $E_{\text{sym}}^2(\rho)$  is the contribution of the first-order symmetry potential  $U_{\text{sym},1}$ . Similarly, for the density slope parameter  $L$  at an arbitrary density  $\rho$ , one can obtain five terms with different characteristics [11–13], i.e.,

$$L(\rho) = L_1(\rho) + L_2(\rho) + L_3(\rho) + L_4(\rho) + L_5(\rho), \quad (17)$$

with

$$L_1(\rho) = \frac{k_F^2}{3m} + \frac{k_F}{6} \frac{\partial U_0(\rho, |\mathbf{k}|, \mathcal{E})}{\partial |\mathbf{k}|} \Big|_{k_F} + \frac{k_F}{6} \frac{\partial \mathcal{E}}{\partial |\mathbf{k}|} \cdot \frac{\partial U_0(\rho, |\mathbf{k}|, \mathcal{E})}{\partial \mathcal{E}} \Big|_{k_F}, \quad (18)$$

$$L_2(\rho) = \frac{k_F^2}{6} \frac{\partial^2 U_0(\rho, |\mathbf{k}|, \mathcal{E})}{\partial |\mathbf{k}|^2} \Big|_{k_F} + \frac{k_F^2}{6} \left\{ \frac{\partial^2 \mathcal{E}}{\partial |\mathbf{k}|^2} \cdot \frac{\partial U_0(\rho, |\mathbf{k}|, \mathcal{E})}{\partial \mathcal{E}} + \left( \frac{\partial \mathcal{E}}{\partial |\mathbf{k}|} \right)^2 \cdot \frac{\partial^2 U_0(\rho, |\mathbf{k}|, \mathcal{E})}{\partial^2 \mathcal{E}} \right\} \Big|_{k_F}, \quad (19)$$

$$L_3(\rho) = \frac{3}{2} U_{\text{sym},1}(\rho, |\mathbf{k}|, \mathcal{E}) \Big|_{k_F}, \quad (20)$$

$$L_4(\rho) = k_F \left[ \frac{\partial U_{\text{sym},1}(\rho, |\mathbf{k}|, \mathcal{E})}{\partial |\mathbf{k}|} + \frac{\partial \mathcal{E}}{\partial |\mathbf{k}|} \cdot \frac{\partial U_{\text{sym},1}(\rho, |\mathbf{k}|, \mathcal{E})}{\partial \mathcal{E}} \right] \Big|_{k_F}, \quad (21)$$

$$L_5(\rho) = 3U_{\text{sym},2}(\rho, |\mathbf{k}|, \mathcal{E}) \Big|_{k_F}. \quad (22)$$

The above expressions clearly show what physics ingredients determine the density dependence of the symmetry energy. More specifically, the  $L_1(\rho)$  represents the kinetic contribution (including the effect from the isoscalar nucleon effective mass), the  $L_2(\rho)$  is due to the momentum dependence of the isoscalar nucleon effective mass, the  $L_3(\rho)$  is directly from the first-order symmetry potential  $U_{\text{sym},1}$ , the  $L_4(\rho)$  relates to the momentum dependence of the  $U_{\text{sym},1}$ , and the  $L_5(\rho)$  is from the second-order symmetry potential  $U_{\text{sym},2}$ .

### C. The nuclear optical model potential and the symmetry potential in asymmetric nuclear matter

In order to obtain the values of the symmetry energy  $E_{\text{sym}}(\rho)$  and the slope parameter  $L(\rho)$  at saturation density  $\rho_0$ , one needs information about the energy (momentum) dependence of the single-nucleon potential, i.e.,  $U_0$ ,  $U_{\text{sym},1}$ ,  $U_{\text{sym},2}$  in asymmetric nuclear matter at  $\rho_0$ . The  $U_0$ ,  $U_{\text{sym},1}$ , and  $U_{\text{sym},2}$  at  $\rho_0$  can be obtained from the real part of the central potential in the optical model, i.e.,  $\mathcal{U}_0(\mathcal{E})$ ,  $\mathcal{U}_{\text{sym},1}(\mathcal{E})$ , and  $\mathcal{U}_{\text{sym},2}(\mathcal{E})$ . In the following, we briefly describe the connection between  $U_0$ ,  $U_{\text{sym},1}$ ,  $U_{\text{sym},2}$  in asymmetric nuclear matter and  $\mathcal{U}_0(\mathcal{E})$ ,  $\mathcal{U}_{\text{sym},1}(\mathcal{E})$ , and  $\mathcal{U}_{\text{sym},2}(\mathcal{E})$  in the optical model.

Both the single-particle potential  $U_n$  of a neutron in asymmetric nuclear matter and the real part of the central potential  $\mathcal{U}_n$  in neutron OMP can be expanded as a power series of  $\delta$  as

$$\Gamma_n = \Gamma_0 + \Gamma_{\text{sym},1} \delta + \Gamma_{\text{sym},2} \delta^2 + \dots \quad (\Gamma = U, \mathcal{U}) \quad (23)$$

The neutron single-particle energy in asymmetric nuclear matter satisfies the following dispersion relation

$$\mathcal{E}_n = T_n + U_n(T_n), \quad (24)$$

where  $\mathcal{E}_n$ ,  $T_n$  and  $U_n(T_n)$  denote the single-neutron energy, the kinetic energy and the potential energy, respectively. In symmetric nuclear matter, the single-neutron energy is

$$\mathcal{E} = T + U_0(T). \quad (25)$$

Following Ref. [23], by expanding Eq. (24) in the power series of  $\delta$  to the second-order and using Eq. (23) and Eq. (25), one can easily obtain

$$U_0 = \mathcal{U}_0, \quad U_{\text{sym},1} = \frac{\mathcal{U}_{\text{sym},1}}{\mu}, \\ U_{\text{sym},2} = \frac{\mathcal{U}_{\text{sym},2}}{\mu} + \frac{\zeta \mathcal{U}_{\text{sym},1}}{\mu^2} + \frac{\vartheta \mathcal{U}_{\text{sym},1}^2}{\mu^3}, \quad (26)$$

with

$$\mu = 1 - \frac{\partial \mathcal{U}_0}{\partial \mathcal{E}}, \quad \zeta = \frac{\partial \mathcal{U}_{\text{sym},1}}{\partial \mathcal{E}}, \quad \vartheta = \frac{\partial^2 \mathcal{U}_{\text{sym},1}}{\partial \mathcal{E}^2}. \quad (27)$$

The relations of  $U_0 = \mathcal{U}_0$  and  $U_{\text{sym},1} = \frac{\mathcal{U}_{\text{sym},1}}{\mu}$  were firstly derived in Ref. [23].

## III. RESULTS AND DISCUSSIONS

The detailed method for obtaining the optimal OMP parameters can be found, e.g., in Refs. [22, 24, 25]. All of the relevant experimental data used in this work are summarized in Ref. [22]. In particular, the original database for searching the global neutron OMP parameters are taken from Table I in Ref. [22]. To see the magnitude

TABLE I: The parameters  $V_i$  and  $W_{vi}$  ( $i = 0, 1, 2, 3, 3L, 4, 4L$ ) as well as  $W_{si}$  ( $i = 0, 1, 2, 3, 3L$ ) obtained directly using all the data in the original database in Ref. [22].

parameter	value	parameter	value
$V_0(\text{MeV})$	55.306	$W_{v0}(\text{MeV})$	-1.7064
$V_1$	-0.341	$W_{v1}$	0.203038
$V_2(\text{MeV}^{-1})$	$4.43 \times 10^{-4}$	$W_{v2}(\text{MeV}^{-1})$	$-7.21 \times 10^{-4}$
$V_3(\text{MeV})$	-20.051	$W_{v3}(\text{MeV})$	$-7.19 \times 10^{-4}$
$V_{3L}$	0.236	$W_{v3L}$	0.209
$V_4(\text{MeV})$	-9.431	$W_{v4}(\text{MeV})$	$-6.12 \times 10^{-5}$
$V_{4L}$	$3.088 \times 10^{-5}$	$W_{v4L}$	$1.24 \times 10^{-6}$
$W_{s0}(\text{MeV})$	12.178	$W_{s2L}$	$2.40 \times 10^{-2}$
$W_{s1}$	-0.2302	$W_{s3}(\text{MeV})$	$-6.63 \times 10^{-6}$
$W_{s2}(\text{MeV})$	-19.025	$W_{s3L}$	$1.04 \times 10^{-5}$

of the isospin dependent second order terms in  $V_v$ ,  $W_s$  and  $W_v$ , we firstly obtain the optimal OMP parameters directly using all the data in the original database in Ref. [22], and the results for the parameters  $V_i$  and  $W_{vi}$  ( $i = 0, 1, 2, 3, 3L, 4, 4L$ ) as well as  $W_{si}$  ( $i = 0, 1, 2, 3, 3L$ ) are listed in Table I. One can see that while the isospin dependent second order terms in  $V_v$  are significant, they are negligibly small in  $W_s$  and  $W_v$ .

In order to evaluate the error of the OMP parameters, we use the Monte Carlo method, i.e., randomly sample 10% of the total experimental data in the original database to form a new searching database, from the latter we then obtain a new set of the OMP parameters. This procedure is repeated 1000 times, and the average values of the OMP parameters and the corresponding errors are then evaluated statistically. In the Monte Carlo estimate, we have neglected the isospin dependent second order terms in  $W_s$  and  $W_v$  since they have essentially no effect on our results.

TABLE II: The average values and the corresponding variances (errors) for the parameter  $V_i$  ( $i = 0, 1, 2, 3, 3L, 4, 4L$ ) obtained from 1000 samples of OMP parameters sets. The  $V_i$  values in Ref. [22] are also included for comparison.

parameter	average value	variance	Ref. [22]
$V_0(\text{MeV})$	55.415	0.3316	54.983
$V_1$	-0.337	$1.163 \times 10^{-2}$	-0.328
$V_2(\text{MeV}^{-1})$	$3.93 \times 10^{-4}$	$1.741 \times 10^{-4}$	$3.10 \times 10^{-4}$
$V_3(\text{MeV})$	-20.107	1.6044	-18.495
$V_{3L}$	0.236	$6.298 \times 10^{-2}$	0.219
$V_4(\text{MeV})$	-9.368	1.6296	-
$V_{4L}$	$3.088 \times 10^{-5}$	$1.3938 \times 10^{-4}$	-

Shown in Table II are the average values and variances (errors) of the parameters  $V_i$  ( $i = 0, 1, 2, 3, 3L, 4, 4L$ ) obtained using the 1000 samples of the OMP parameter sets. For comparison, we also include in Table II the  $V_i$  values of Ref. [22] where the higher-order terms

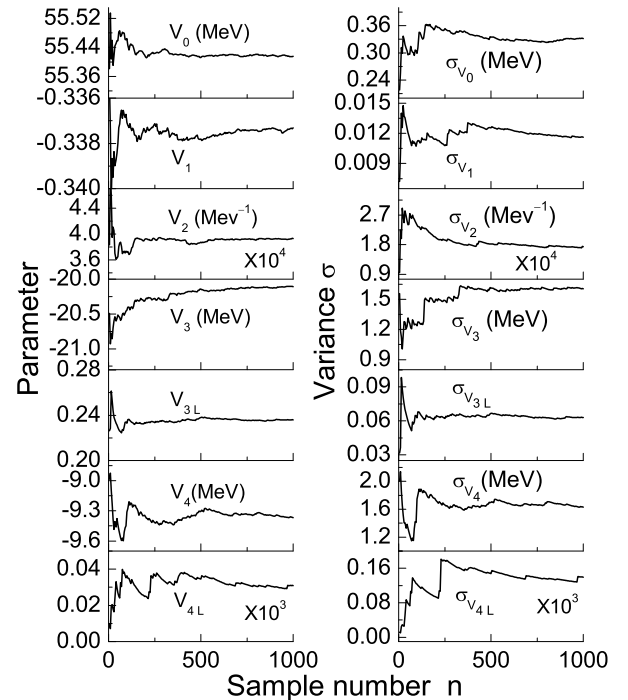


FIG. 1: The average values and variances (errors) of the parameters  $V_i$  ( $i = 0, 1, 2, 3, 3L, 4, 4L$ ) as a function of the sample number  $n$  of OMP parameters sets.

$V_i$  ( $i = 4, 4L$ ) were neglected. One can see that including the higher-order terms  $V_i$  ( $i = 4, 4L$ ) enhances the magnitude of the  $V_i$  ( $i = 3, 3L$ ) although the average values of  $V_i$  ( $i = 0, 1, 2, 3, 3L$ ) are still consistent with the values obtained directly from all the data in the original database in Ref. [22] without  $V_i$  ( $i = 4, 4L$ ). To be more clear, the average values and variances of  $V_i$  ( $i = 0, 1, 2, 3, 3L, 4, 4L$ ) are also shown in Fig. 1 as a function of the sample number  $n$  of the OMP parameters sets. It is seen that both the average values and the variances have all well converged at  $n = 1000$ .

Shown in Fig. 2 is the energy dependence of the single-nucleon isoscalar potential  $U_0$  ( $\mathcal{U}_0$ ) obtained from our OMP parameters. For comparison, the results of the Schrödinger equivalent potential obtained by Hama *et al* [26] from the nucleon-nucleus scattering data based on the Dirac phenomenology are also shown. It is seen clearly that our isoscalar potential is in good agreement with that from the Dirac phenomenology. We limit the comparison up to 200 MeV since the experimental data of the neutron-nucleus elastic scattering angular distributions used in the present work is in the beam energy range of about 0 – 200 MeV [22].

From the OMP parameters  $V_i$  ( $i = 0, 1, 2, 3, 3L, 4, 4L$ ), we can first obtain the energy (momentum) dependence of the  $\mathcal{U}_{\text{sym},1}$  and  $\mathcal{U}_{\text{sym},2}$ , and then the energy (momentum) dependence of  $U_{\text{sym},1}$  and  $U_{\text{sym},2}$  using Eq. (26). Shown in Fig. 3 is the momentum dependence of  $\mathcal{U}_{\text{sym},1}$ ,  $\mathcal{U}_{\text{sym},1}$ ,  $\mathcal{U}_{\text{sym},2}$ , and  $U_{\text{sym},2}$ . One can see that the  $U_{\text{sym},1}$  is

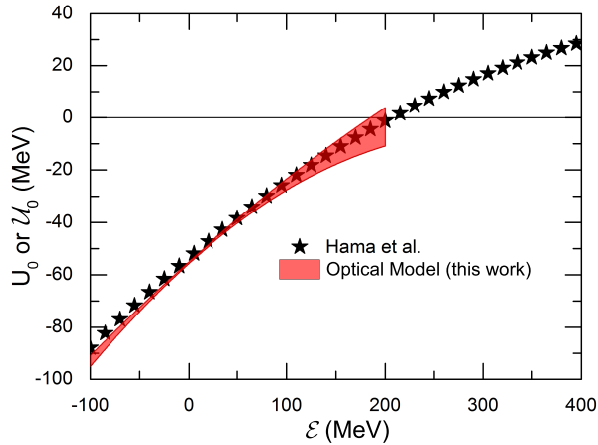


FIG. 2: (Color online) Energy dependence of single-nucleon potential  $U_0$  ( $\mathcal{U}_0$ ) in symmetric nuclear matter obtained from our OMP parameters. The results of the Schrödinger equivalent potential obtained by Hama *et al* [26] from the nucleon-nucleus scattering data are also included for comparison.

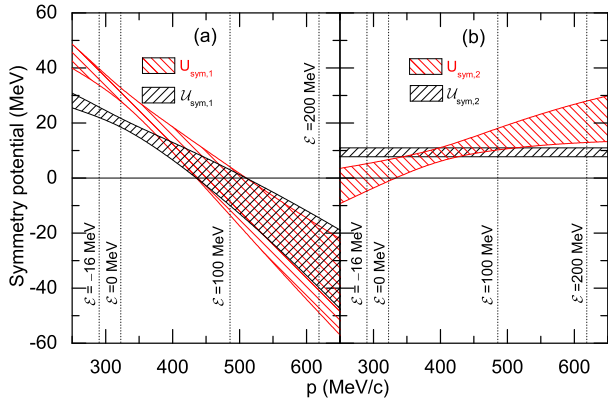


FIG. 3: (Color online) Momentum dependence of  $U_{\text{sym},1}$  ( $U_{\text{sym},1}$ ) (a) and  $U_{\text{sym},2}$  ( $U_{\text{sym},2}$ ) (b). The corresponding momenta at  $\mathcal{E} = -16, 0, 100$  and  $200$  MeV are indicated by dotted lines.

larger than the  $U_{\text{sym},1}$  at lower momenta (energies) while the  $U_{\text{sym},1}$  becomes smaller than the  $U_{\text{sym},1}$  at higher momenta (energies). This feature is qualitatively consistent with the results in Ref. [23]. In addition, both the  $U_{\text{sym},1}$  and  $U_{\text{sym},1}$  decrease with nucleon momentum  $p$  and become negative when the nucleon momentum is larger than about  $p = 470$  MeV/c (i.e.,  $\mathcal{E} = 90$  MeV). These are in qualitative agreement with the previous results [11, 27–29]. Furthermore, it is interesting to see that while the  $U_{\text{sym},2}$  is almost a constant, the  $U_{\text{sym},2}$  increases with the nucleon momentum  $p$  due to the transformation relation in Eq. (26). Our results indicate that the magnitude of the  $U_{\text{sym},2}$  at  $\rho_0$  can be comparable with that of the  $U_{\text{sym},1}$ , especially at higher energies. These features may be useful for constraining the model parameters of isospin-dependent nuclear effective interactions.

From the  $U_{\text{sym},1}$  and  $U_{\text{sym},2}$  at  $\rho_0$  together with the em-

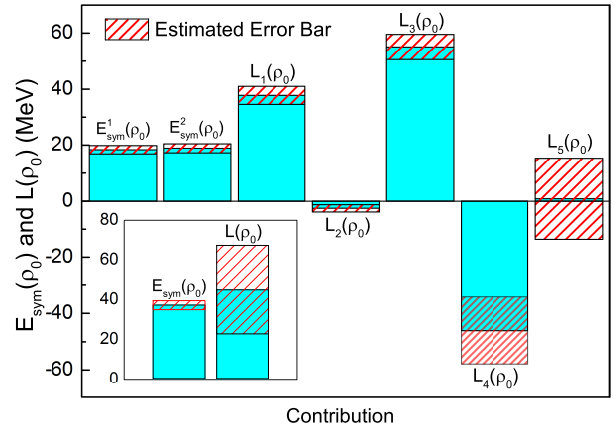


FIG. 4: (Color online) Contributions of each term in the decompositions of Eq. (14) and Eq. (17) for  $E_{\text{sym}}(\rho_0)$  and  $L(\rho_0)$ . The inset shows the results for  $E_{\text{sym}}(\rho_0)$  and  $L(\rho_0)$ .

piral properties of symmetric nuclear matter at saturation density, i.e.  $\rho_0 = 0.16 \pm 0.02 \text{ fm}^{-3}$  and  $\mathcal{E}_0 = -16 \pm 0.5$  MeV, the two contributions to the symmetry energy are found to be  $E_{\text{sym}}^1(\rho_0) = 18.36 \pm 1.49$  MeV and  $E_{\text{sym}}^2(\rho_0) = 18.88 \pm 1.62$  MeV, respectively. The five terms contributing to the slope parameter  $L(\rho_0)$  are, respectively,  $L_1(\rho_0) = 37.76 \pm 3.23$  MeV,  $L_2(\rho_0) = -2.57 \pm 1.29$  MeV,  $L_3(\rho_0) = 55.08 \pm 4.48$  MeV,  $L_4(\rho_0) = -46.11 \pm 11.87$  MeV, and  $L_5(\rho_0) = 0.81 \pm 14.48$  MeV. These different contributions are also shown in Fig. 4 together with the  $E_{\text{sym}}(\rho_0)$  and  $L(\rho_0)$ . The resulting total symmetry energy and its density slope at  $\rho_0$  are, respectively,

$$E_{\text{sym}}(\rho_0) = 37.24 \pm 2.26 \text{ MeV}, \quad (28)$$

$$L(\rho_0) = 44.98 \pm 22.31 \text{ MeV}. \quad (29)$$

While they are well consistent with the available constraints, the  $L(\rho_0)$  is closer to the lower end while the  $E_{\text{sym}}(\rho_0)$  is closer to the upper end of the range covered by previous results obtained from analyzing many other observables using various methods (See, e.g., Refs. [5–9]).

For the decomposition of  $L(\rho_0)$ , it is seen that the magnitude of  $L_2(\rho_0)$  is very small, indicating that the contribution of the momentum dependence of the isoscalar nucleon effective mass is unimportant, consistent with the theoretical calculations in Ref. [13] and the assumption made in Ref. [11]. On the other hand, the  $L_4(\rho_0)$  contributes a significant negative value to  $L(\rho_0)$ , demonstrating the importance of the momentum dependence of the first-order symmetry potential  $U_{\text{sym},1}$  which is related to the isovector nucleon effective mass [11]. In addition, it is interesting to see that the magnitude of  $L_5(\rho_0)$  is quite small, consistent with the assumption made in Ref. [11] where the  $L_5(\rho_0)$ , i.e., the contribution of the second-order symmetry potential  $U_{\text{sym},2}$  was neglected. The smallness of  $L_5(\rho_0)$  is due to the fact that the  $U_{\text{sym},2}$  essentially vanishes around  $\mathcal{E} = -16$  MeV as shown in Fig. 3 (b). However, it should be noted that the  $L_5(\rho_0)$  has a large uncertainty, and actually it contributes the



main part of the uncertainty of  $L(\rho_0)$ . One can see from Fig. 4 that more precise information on the momentum dependence of  $U_{\text{sym},1}$  and the magnitude of  $U_{\text{sym},2}$  at the single-nucleon energy of  $\mathcal{E}_0 = -16 \pm 0.5$  MeV is necessary to reduce the uncertainties of the  $L(\rho_0)$ .

In the above evaluation of the  $E_{\text{sym}}(\rho_0)$  and  $L(\rho_0)$ , the empirical values of  $\rho_0 = 0.16 \pm 0.02 \text{ fm}^{-3}$  and  $\mathcal{E}_0 = -16 \pm 0.5$  MeV have been used. According to the HVH theorem, the  $\mathcal{E}_0$  and  $\rho_0$  should be related to each other if the  $U_0(\mathcal{E})$  is known. Using  $\rho_0 = 0.16 \pm 0.02 \text{ fm}^{-3}$  and the  $U_0(\mathcal{E})$  extracted in the present work, we obtain  $\mathcal{E}_0 = -28.52 \pm 4.85$  MeV,  $E_{\text{sym}}(\rho_0) = 40.12 \pm 2.84$  MeV and  $L(\rho_0) = 44.61 \pm 24.40$  MeV. It is seen that the value of  $\mathcal{E}_0 = -28.52 \pm 4.85$  MeV significantly deviates from the empirical value and this seems to be a common problem for usual phenomenological optical model potentials (See, e.g., Ref. [17–22, 30]). Fortunately, the extracted value of  $L(\rho_0)$  and its single-nucleon potential decomposition essentially do not change although the  $E_{\text{sym}}(\rho_0)$  increases by about 3 MeV compared to the results using the empirical values of  $\rho_0 = 0.16 \pm 0.02 \text{ fm}^{-3}$  and  $\mathcal{E}_0 = -16 \pm 0.5$  MeV.

#### IV. SUMMARY AND OUTLOOK

In summary, using the available experimental data from neutron-nucleus scatterings, we first obtained a new set of the global isospin dependent neutron-nucleus optical model potential parameters which include the nuclear symmetry potential up to the second order in isospin asymmetry for the first time. Using the analytical relationship between the single-nucleon potentials in asymmetric nuclear matter and the optical model potentials, we then evaluated both the first-order and the second-order symmetry potentials  $U_{\text{sym},1}$  and  $U_{\text{sym},2}$  in asymmetric nuclear matter at saturation density. It is found that the strength of the  $U_{\text{sym},2}$  is significant compared to that of the  $U_{\text{sym},1}$ , especially at high nucleon momentum. Moreover, while the  $U_{\text{sym},1}$  decreases with nucleon momentum, the  $U_{\text{sym},2}$  displays an opposite behavior. It will be interesting to investigate effects of the  $U_{\text{sym},2}$  in heavy ion collisions induced by neutron-rich nuclei at intermediate energies. The extracted  $U_{\text{sym},1}$  and  $U_{\text{sym},2}$  together with the empirical values of  $\rho_0 = 0.16 \pm 0.02 \text{ fm}^{-3}$  and  $\mathcal{E}_0 = -16 \pm 0.5$  MeV were then used to evaluate the nuclear symmetry energy and its density slope at saturation density by applying the formulas derived earlier based on the HVH theorem. We found that the neutron-nucleus scattering data lead to a value of  $E_{\text{sym}}(\rho_0) = 37.24 \pm 2.26$  MeV and  $L(\rho_0) = 44.98 \pm 22.31$  MeV, respectively, consis-

tent with the results obtained from analyzing many other observables within various models. Furthermore, our results indicate that the contribution of the second-order symmetry potential to the  $L(\rho_0)$  is quite small, though with a large uncertainty, verifying the assumption made in Ref. [11].

To evaluate the  $E_{\text{sym}}(\rho_0)$  and  $L(\rho_0)$  from the single-nucleon potentials in asymmetric nuclear matter, one needs information about the optical model potentials at negative energies, e.g.,  $\mathcal{E}_0 = -16 \pm 0.5$  MeV. In this work, this was done by extrapolating the optical model parameters obtained from analyzing the neutron-nucleus scattering data in the beam energy region of 0–200 MeV. The extrapolation may lead to uncertainties in extracting the symmetry energy and its slope parameter. To be more accurate, one may use the dispersive optical model [31–35] in which the real and imaginary parts of the optical model potential are connected with each other by a dispersive integration, and the optical model potentials can thus be extended to negative energies to address simultaneously the bound single-particle properties as well as elastic nucleon scattering. Using the dispersive optical model for elastic nucleon scattering data and the bound-state data of finite nuclei, one expects to obtain more reliable information about the optical model potentials at negative energies. It would be interesting to see how our present results change if the dispersive optical model is used. These studies are in progress and will be reported elsewhere.

#### Acknowledgments

One of us (X.H. Li) would like to thank Professors Chong-Hai Cai, Qing-Biao Shen and Yin-Lu Han for useful discussions. This work was supported in part by the NNSF of China under Grant Nos. 10975097, 11047157, 11135011, 11175085, 11275125, 11205083, and 11235001, the Shanghai Rising-Star Program under grant No. 11QH1401100, the “Shu Guang” project supported by Shanghai Municipal Education Commission and Shanghai Education Development Foundation, the Program for Professor of Special Appointment (Eastern Scholar) at Shanghai Institutions of Higher Learning, the Science and Technology Commission of Shanghai Municipality (11DZ2260700), the US National Aeronautics and Space Administration under grant NNX11AC41G issued through the Science Mission Directorate, and the US National Science Foundation under Grant No. PHY-1068022.

- 
- [1] B.A. Li, C.M. Ko, and W. Bauer, *Int. J. Mod. Phys. E* **7**, 147 (1998).  
 [2] V. Baran, M. Colonna, V. Greco, and M. Di Toro, *Phys.*

- Rep.* **410**, 335 (2005).  
 [3] A.W. Steiner, M. Prakash, J.M. Lattimer, and P.J. Ellis, *Phys. Rep.* **411**, 325 (2005).

- [4] L.W. Chen, C.M. Ko, B.A. Li, and G.C. Yong, *Front. Phys. China* **2**, 327 (2007).
- [5] B.A. Li, L.W. Chen, and C. M. Ko, *Phys. Rep.* **464**, 113 (2008).
- [6] B.M. Tsang et al., *Phys. Rev. C* **86**, 015803 (2012).
- [7] J.M. Lattimer, *Annu. Rev. Nucl. Part. Sci.* **62**, 485 (2012).
- [8] L.W. Chen, arXiv:1212.0284, 2012.
- [9] B.A. Li, L.W. Chen, F.J. Fattoyev, W. G. Newton, and C. Xu, arXiv:1212.1178, 2012.
- [10] N.M. Hugenholtz and L. Van Hove, *Physica* **24**, 363 (1958).
- [11] C. Xu, B.A. Li, and L.W. Chen, *Phys. Rev. C* **82**, 054607 (2010).
- [12] C. Xu, B.A. Li, L.W. Chen, and C.M. Ko, *Nucl. Phys.* **A865**, 1 (2011).
- [13] R. Chen, B.J. Cai, L.W. Chen, B.A. Li, X.H. Li, and C. Xu, *Phys. Rev. C* **85**, 024305 (2012).
- [14] B.J. Cai and L.W. Chen, *Phys. Lett.* **B711**, 104 (2012).
- [15] A.M. Lane, *Nucl. Phys.* **35**, 676 (1962).
- [16] P.G. Yong, *RIPL Handbook*, Vol. 41, 1998, <http://www-nds.iaea.org/ripl/>, Chapter 4: Optical Model Parameters.
- [17] A.J. Koning and J.P. Delaroche, *Nucl. Phys.* **A713**, 231 (2003).
- [18] F.D. Becchetti and G.W. Greenless, *Phys. Rev.* **182**, 1190 (1969).
- [19] R.L. Varner, W.J. Thompson, T.L. Mcabee, E.J. Ludwig, and T.B. Clegg, *Phys. Rep.* **201**, 57 (1991).
- [20] S.P. Weppner, R.B. Penney, G.W. Diffendale, and G. Vittorini, *Phys. Rev. C* **80**, 034608 (2009).
- [21] Y.L. Han, Y.L. Xu, H.Y. Liang, H.R. Guo, and Q.B. Shen, *Phys. Rev. C* **81**, 024616 (2010).
- [22] X.H. Li and L.W. Chen, *Nucl. Phys. A* **874**, 62 (2012).
- [23] J. Dabrowski, *Phys. Lett.* **8**, 90 (1964).
- [24] X.H. Li, C.T. Liang, and C.C. Hai, *Nucl. Phys.* **A789**, 103 (2007).
- [25] Q.B. Shen, *Nucl. Sci. Eng.* **141**, 78 (2002).
- [26] S. Hama, B.C. Clark, E.D. Cooper, H.S. Sherif, and R.L. Mercer, *Phys. Rev. C* **41**, 2737 (1990).
- [27] B.A. Li, *Phys. Rev. C* **69**, 064602 (2004).
- [28] L.W. Chen, C.M. Ko, and B.A. Li, *Phys. Rev. C* **72**, 064606 (2005).
- [29] Z.H. Li, L.W. Chen, C.M. Ko, B.A. Li, and H.R. Ma, *Phys. Rev. C* **74**, 044613 (2006).
- [30] J.P. Jeukenne, A. Lejeune, and C. Mahaux, *Phys. Rep.* **25**, 83 (1976).
- [31] C. Mahaux and H. Ngô, *Nucl. Phys. A* **431**, 486 (1984).
- [32] C. Mahaux and R. Sartor, *Nucl. Phys. A* **468**, 193 (1987).
- [33] R.J. Charity, L.G. Sobotka, and W.H. Dickhoff, *Phys. Rev. Lett.* **97**, 162503 (2006).
- [34] R.J. Charity, J.M. Mueller, L.G. Sobotka, and W.H. Dickhoff, *Phys. Rev. C* **76**, 044314 (2007).
- [35] X.H. Li and C.H. Cai, *Nucl. Phys.* **A801**, 43 (2008).